Check for updates

Accepted Article

On the Use of Machine Learning Techniques for the Mechanical Characterization of Soft Biological Tissues

M. Cilla[1,2,3], I. Pérez-Rey[4], M.A. Martínez[2,3], E. Peña[2,3], J. Martínez[4,5]

[1]*Centro Universitario de la Defensa (CUD), Academia General Militar(AGM), Zaragoza, Spain*

[2]*Aragon Institute of Engineering Research (I3A), University of Zaragoza, Zaragoza, Spain*

[3]*CIBER's Bioengineering, Biomaterials and Nanomedicine (CIBER-BBN), Spain*

[4]*Centro Universitario de la Defensa (CUD), Escuela Naval Militar, Martin, Spain*

SUMMARY

Motivated by the search for new strategies for fitting a material model, a new approach is explored in the present work. The use of numerical and complex algorithms based on machine learning techniques such as support vector machines for regression, bagged decision trees and artificial neural networks is proposed for solving the parameter identification of constitutive laws for soft biological tissues. First, the mathematical tools were trained with analytical uniaxial data (circumferential and longitudinal directions) as inputs, and their corresponding material parameters of the Gasser, Ogden and Holzapfel strain energy function as outputs. The train and test errors show great efficiency during the training process in finding correlations between inputs and outputs; besides, the correlation coefficients were very close to 1. Second, the tool was validated with unseen observations of analytical circumferential and longitudinal uniaxial data. The results show an excellent agreement between the prediction of the material parameters of the SEF and the analytical curves. Finally, data from real circumferential and longitudinal uniaxial tests on different cardiovascular tissues were fitted, thus the material model of these tissues was predicted. We found that the method was able to consistently identify model parameters, and we believe that the use of these numerical tools could lead to an improvement in the characterization of soft biological tissues.

Received ...

KEY WORDS: Artificial Neural Network, Support Vector Machine, Bagged Decision Trees, Machine Learning Techniques, soft tissue, mechanical test, strain energy function, uniaxial test, material properties.

*Correspondence to: *J. Martnez, Plaza de Espaa s/n, 36920. Marn (Pontevedra) javier.martinez@cud.uvigo.es

This article has been accepted for publication and undergone full peer review but has not been through the copyediting, typesetting, pagination and proofreading process, which may lead to differences between this version and the Version of Record. Please cite this article as Int. J. Numer. Meth. Biomed. Engng., e03121. doi: 10.1002/cnm.3121

1. INTRODUCTION

The experimental study of the mechanical properties of biological tissues is vitally important. Research into the mechanical response of biological tissues and organs is the basis for the creation of computational models which can accurately reproduce their mechanical behaviour. In order to obtain the material properties of these tissues, classical engineering testing techniques have been applied to biological materials [**?**, see e.g.,]and references therein]Fung1979,Fung1990,Humphrey2001. Specifically, the characterization of the mechanical properties of soft biological tissues, such as blood vessels, is especially challenging due to the particular characteristics of these tissues (anisotropy, incompressibility, active and passive behaviour or presence of residual stresses), which noticeably complicate the obtaining of valid results. For this reason, the experimental study of soft biological tissues is one of the fields of biomechanics in which more research effort is required. In particular, the huge variability in the mechanical response of vascular tissues is one of the most serious difficulties in the determination of their mechanical properties. Due to the different physiological role of each vessel and the different mechanical loading they are subjected to, their mechanical properties are highly variable [1, 2].

In the testing procedures used for the characterization of the mechanical properties of soft biological tissues, such as blood vessels, three different techniques are mainly used for the measurement of their mechanical response; simple tension, planar biaxial and inflation tests. Of these, the uniaxial test is the easiest and therefore the most commonly used for the mechanical characterization of soft tissues. This type of test, widely used for the determination of the mechanical properties of all kinds of materials, has been applied to soft biological tissues [**?**, see, e.g.,]]Hayashi1981,Hayashi1997,Schulze-Bauer2003,Holzapfel2005a. Among its main advantages, it is worth noting its simplicity and versatility, which allows its application to very small samples. Nevertheless, it allows obtaining the mechanical properties only in the testing directions. This is irrelevant when dealing with isotropic materials, but it is an important shortcoming in testing anisotropic materials. A feasible possibility to complete the information provided by simple tension tests is to apply them to different tension directions [8], which partly compensates for this limitation. This kind of test involves gripping a sample specimen at both ends and pulling it at a specified rate until the sample breaks. During the test, the force is recorded as a function of elongation, and then the mechanical behavior of the tissue is extracted. By considering the dimensions of the sample, it is possible to determine the properties of the biological material.

In the context of mathematical modelling and computational simulations, the experimental data are usually used to estimate the material model parameters through a strain energy function (SEF)

Accepted Article

within the framework of the continuum theory of large deformation hyperelasticity. In recent years, the constitutive modelling of soft biological tissues has constituted a very active field of research [**?**, see, e.g.,]]Ogden2003. These materials have commonly been modelled as hyperelastic continua embedded into continuum mechanical formulations. Accordingly, one of the main tasks consists of the determination of appropriate strain energy density functions, from which local mechanical quantities are derived [10]. Many constitutive laws have been proposed for soft tissue modelling [**?**, see e.g.,]]Demiray1972,Fung1979,Humphrey1987,Weiss1996 which would be suitable or not depending on the kind of soft biological tissue in question. For instance, the most common SEFs for modelling the behaviour of blood vessels are the models developed by Holzapfel *et. al* [14, 8], which account for two preferred directions and incorporate fibre dispersion with respect to the deterministic preferred orientation direction, and the more recent work by Gasser *et. al* [15], which includes microstructural information in the model by means of the assumption of a fibre orientation distribution function.

Nevertheless, apart from the relevant features of the soft biological tissues, the type of mechanical test and their conditions, or the selected SEF for modelling the behaviour of the tissue, there are also differences in the methods that can be used to determine the coefficients of a material model. Traditionally, material parameters associated with the material model have been fitted by means of a Levenberg-Marquardt type minimization algorithm [16] and/or inverse models combined with Finite Element (FE) models [17]. Although significant advances have been made in the prediction of mechanical parameters of soft biological tissues, there is still much work left to be done since these and other implementations have, in general, made use of numerical gradients. Numerical gradients are limited to local optimization and are thus very dependent on the initial seed, which is a number or vector used to initialize the numerical algorithm, minimizing their reliability and efficiency. In addition, for each experimental test, a new fitting and a good choice of a seed should be made, which sometimes leads to an elaborate process. As a result of the constant search for effective solutions to the problem of the parameter fitting of soft biological tissues, the present study proposes the use of Machine Learning Techniques (MLTs) such as Support Vector Machines (SVMs), Bagged (Bootstrap-Aggregated) Decision Trees (BDT) or Artificial Neural Networks (ANNs). MLTs explore the development of algorithms that can learn and make predictions from data. These techniques are characterized by complex algorithms that can be trained to reproduce the behaviour of a model [18, 19]. In technical fields such as mathematics, engineering, computer science or statistics, the multidisciplinary nature of MLTs is highlighted by their applicability to many different areas, such as electronics [**?**, see e.g.,]]Jabbour1987, industry [**?**, see e.g.,]]Evans1992, geology [**?**, see e.g.,]]Taboada2007,Lopez2010b, space science [**?**, see e.g.,]]Fayyad1993, or language [**?**, see e.g.,]]Liu2005 amongst many others. Within the biomedical

Accepted Article

context, these techniques have also been successfully applied to several clinical applications, for instance interpreting electrocardiograms, diagnosis of breast cancer or melanomas, predicting femur loads or optimized hip implant geometries [**?**, see e.g.,]]Handels1999,Gniadecka2004,Huang2005, Garijo2014, Cilla2017. They have also been used for treating cardiovascular diseases [**?**, see e.g.,]]Poli1991,ltchhaporia1995,Itchhaporia1996, MCilla2011, LiangL2017.

The goal of this study is to develop a tool, using MLTs, to estimate the material parameters of a SEF in a fast and efficient way. Once the tool is trained, a new fitting is immediate and the response time is negligible. Specifically, we have focused on the mechanical characterization of blood vessels by means of the SEF proposed by Gasser *et. al* [15]. In addition, this methodology has been proposed for the most common experimental test for blood vessels, that is, the uniaxial test.

2. MECHANICAL CHARACTERIZATION OF BLOOD VESSELS

In this section, we summarize briefly the equations of incompressible non-linear elasticity that are required for comparing the theory with experimental data in standard uniaxial experimental protocols for the characterization of blood vessels.

2.1. Pure homogeneous uniaxial test

We consider homogeneous deformations that can be classified as pure homogeneous strain, that is, deformations of the form

$$x_1 = \lambda_1 X_1, \qquad x_2 = \lambda_2 X_2, \qquad x_3 = \lambda_3 X_3, \tag{1}$$

where $(X_1,\ X_2,\ X_3)$ are rectangular Cartesian coordinates that identify material points in the reference configuration, $(x_1,\ x_2,\ x_3)$ are the corresponding coordinates after deformation with respect to the same axes, and $(\lambda_1,\ \lambda_2,\ \lambda_3)$ are the principal stretches of the left Cauchy-Green deformation tensor $\mathbf{C} = \mathbf{F}^{\mathrm{T}} \cdot \mathbf{F}$ with $\mathbf{F} := \nabla_{\mathbf{X}} \boldsymbol{\varphi}(\mathbf{X})$ the two-point deformation gradient tensor. The deformation gradient and the Cauchy stress tensor $\boldsymbol{\sigma}$ in this particular case are defined as

$$\mathbf{F} = \begin{bmatrix} \lambda_1 & 0 & 0 \\ 0 & \lambda_2 & 0 \\ 0 & 0 & \lambda_3 \end{bmatrix} \qquad \boldsymbol{\sigma} = \begin{bmatrix} \sigma_1 & 0 & 0 \\ 0 & \sigma_2 & 0 \\ 0 & 0 & \sigma_3 \end{bmatrix} \tag{2}$$

Furthermore, the principal stretches satisfy the constraint $\lambda_1\lambda_2\lambda_3 = 1$ for an incompressible material. If the deformation of eq. (2.1) is applied to a thin material, a plane stress condition applies

Accepted Article

and we may set $\sigma_3 = 0$, the stress normal to the plane and, for simple uniaxial tension, we set $\sigma_2 = 0$ and $\sigma_1 = \sigma$.

2.2. *Constitutive modelling of blood vessels*

Stress-stretch experimental curves of blood vessels have a high nonlinearity. This fact motivates the use of an exponential function for describing the strain energy stored in the collagen fibers where each family of fibers represents the main direction of collagen bundles that are orientated in a helicoidal manner at $\pm\theta$ degrees, where θ is a phenomenological variable. Both families of fibers were assumed to have the same mechanical response [14].

The Gasser, Ogden and Holzapfel (GOH) model [15] extended the model of Holzapfel *et. al* [14] by the application of generalized structure tensor $\mathbf{H} = \kappa\mathbf{1} + (1 - 3\kappa)\mathbf{M}_0$ (where $\mathbf{1}$ is the identity tensor and $\mathbf{M}_0 = \mathbf{m}_0 \otimes \mathbf{m}_0$ is a structure tensor defined using unit vector $\mathbf{m}_0$ specifying the mean orientation of the fibers) and they come up with a new constitutive model

$$\Psi = \mu[I_1 - 3] + \frac{k_1}{2k_2} \sum_{i=4,6} \exp\left(k_2\left[\kappa[I_1 - 3] + [1 - 3\kappa][I_i - 1]\right]^2\right) - 1, \tag{3}$$

where $\mu > 0$ and $k_1 > 0$ are stress-like parameters and $k_2 > 0$ and $0 \leq \kappa \leq \frac{1}{3}$ are dimensionless parameters (when κ=0 the fibres are perfectly aligned (no dispersion) and when κ=$\frac{1}{3}$ the fibres are randomly distributed and the material becomes isotropic) , $I_1 = tr(\mathbf{C})$ is the first invariant of $\mathbf{C}$, with $\mathbf{C} = \mathbf{F}^T\mathbf{F}$ the right Cauchy-Green tensor and $\mathbf{F}$ the deformation gradient tensor, $I_4(\mathbf{C}, \mathbf{a}_1) = \mathbf{a}_1 \cdot \mathbf{C} \cdot \mathbf{a}_1$ and $I_6(\mathbf{C}, \mathbf{a}_2) = \mathbf{a}_2 \cdot \mathbf{C} \cdot \mathbf{a}_2$ are invariants which depend on the direction of the family of fibres at a material point $\mathbf{X}$ that is defined by the unit vectors field $\mathbf{a}_1$ and $\mathbf{a}_2$ [36]. Finally, the anisotropic invariants are defined by θ angle. It should be noted that it was assumed that the two principal axes of $\mathbf{C}$ coincide with the circumferential and longitudinal directions.

$$I_4 = \lambda_\theta^2 \cos^2(\theta) + \lambda_z^2 \sin^2(\theta), \qquad I_6 = \lambda_\theta^2 \cos^2(-\theta) + \lambda_z^2 \sin^2(-\theta). \tag{4}$$

2.3. *Standard fitting of experimental data*

The most common methods found in the literature for fitting uniaxial experimental data are based on the use of a Levenberg-Marquardt non-linear least square fitting algorithm [16], which typically minimizes the objective function represented by

$$\chi^2 = \Sigma_{i=1}^{n} \left[\left(\sigma_{\theta\theta} - \sigma_{\theta\theta}^{\tilde{\Psi}}\right)_i^2 + \left(\sigma_{zz} - \sigma_{zz}^{\tilde{\Psi}}\right)_i^2 \right], \tag{5}$$

Accepted Article

where n is the number of data points, $\sigma_{\theta\theta}$ and σ_{zz} are the Cauchy (true) stress of the experimental data, $\sigma_{\theta\theta}^{\tilde{\Psi}}$ and $\sigma_{zz}^{\tilde{\Psi}}$ are the Cauchy stresses for the *i*th point computed by the equation

$$\sigma_{ii}^{\Psi} = 2\mu\left[\lambda_i^2 - \frac{1}{\lambda_i}\right] + \frac{k_1}{k_2}\lambda_i e^{k_2\left[[1-\rho]\left[\lambda_i^2+\frac{2}{\lambda_i}-3\right]^2+\rho\left[\lambda_i^2\cos^2\theta+\frac{\sin^2\theta}{\lambda_i}-1\right]^2\right]}$$
$$\left[2k_2[1-\rho]\left[\lambda_i^2+\frac{2}{\lambda_i}-3\right]\left[2\lambda_i-\frac{2}{\lambda_i^2}\right]+2\rho\left[\lambda_i^2\cos^2\theta+\frac{\sin^2\theta}{\lambda_i}-1\right]\left[2\lambda_i\cos^2\theta+\frac{\sin^2\theta}{\lambda_i^2}\right]\right], \tag{6}$$

with $i = z, \theta$ corresponding to the longitudinal and circumferential directions respectively. It is well-known that the problem of these numerical methods based on gradients is their limitation to local optimization, and therefore their instability and dependence on the selected initial seed. This means that many attempts may be requited to get a good fitting.

3. MATHEMATICAL BACKGROUND

Machine Learning Techniques represent a branch of artificial intelligence based on mathematical models able to solve different problems which present a relevant non-linearity [18]. In the present case, three supervised-learning techniques have been selected, namely: Support Vector Machines for Regression, Bagged Decision Trees and Artificial Neural Networks in their most popular version, the so-called Multi-Layer Perceptron (MLP) [37].

3.1. Support Vector Machines for Regression

Support Vector Machines represent a family of supervised-learning methods used both as classification and regression tools, capable of approximating any multivariate function to any level of accuracy. They were initially developed to address classification problems and later extended to solve regression problems [38, 39, 40]. The model produced by a SVR is only dependent on a subset of the training data, because the cost function for building the model ignores any training data that are close (within a threshold ϵ) to the model prediction. Rather than classifying new unseen variables $\overrightarrow{x}$ into one of two categories ($\hat{y}$=$\pm$1), the idea is to predict a real-valued output for y'. Therefore, training data will be of the form $\{\overrightarrow{x}, t_2\}$, where i = 1, 2, ..., L, $y \in \Re$, $\overrightarrow{x} \in \Re^D$:

$$y_i = \overrightarrow{w} \cdot \overrightarrow{x_i} + b \tag{7}$$

Accepted Article

The SVR uses a somewhat more sophisticated penalty function in such a way that the penalty is not imposed if the predicted value y_i is less than a distance ϵ away from the actual value t_i.

3.2. Bagged Decision Trees

Bagging or bootstrap aggregation is usually used when the variance of a decision tree has to be reduced. The combination of results from many decision trees reduces the effects of overfitting and improves generalization. The algorithm selects a random subset of predictors to use at each decision split as in the random forest method [41].

3.3. Multi-Layer Perceptron

ANNs are inspired by biological neural networks such as those encountered in human beings [42]. These algorithms are made up of two main elements: a structure formed by basic units (neurons) and the algorithm used to learn and to be trained. Although, recently studies has been explored other possibilities to facilitate the optimization of neural networks [43], traditional definition of ANN has been implemented in this work, and therefore, the functional model of neural networks implements the function $\mathbf{f} : X \subset \mathbb{R}^d \rightarrow Y \subset \mathbb{R}^c$:

$$\mathbf{f}(\mathbf{x}) = \phi(\psi(\mathbf{x})), \tag{8}$$

$$\psi : \mathbf{X} \subset \mathbb{R}^d \rightarrow T \subset \mathbb{R}^p,$$

$$\phi : \mathbf{T} \subset \mathbb{R}^p \rightarrow Y \subset \mathbb{R}^c,$$

where $\mathbf{X}$ is the input space, $\mathbf{Y}$ is the output space, $\mathbf{T}$ is the hidden space, ψ is the activation function of the hidden layer, and ϕ is the activation function of the input layer. The implemented function for the MLP is

$$f = \sum_{j=1}^{h} \phi_j(c_j\psi)(\mathbf{w}_j^T\mathbf{x}) + w_0 + c_0, \tag{9}$$

where $\mathbf{w}$ and w_0 are the weights of the input layer and $\mathbf{c}$ and c_0 are the weights of the hidden layer.

Accepted Article

3.4. Application of Machine Learning Techniques (MLTs) to the constitutive fitting of uniaxial curves of blood vessels

The use of MLTs for the prediction of material parameters of a SEF is explored in this work. The workflow, which is shown in Figure 1, is divided into two phases: the application and verification stages. According to this figure, data is initially collected from circumferential and longitudinal uniaxial tests carried out on soft biological tissues. 1080 analytical curves, which cover a range of responses from highly anisotropic to quasi-isotropic, were used at this stage. From uniaxial tests, it is possible to recover stress-strain pairs for each longitudinal and circumferential case. The input of the MLT was initially defined in two ways with the purpose of defining an input of the machine learning tool: on the one hand, by fitting a double exponential equation ($ae^{bx} + ce^{dx}$) and, on the other hand, by extracting three customized parameters (initial slope, middle point and final slope) from the stress-strain curves. This kind of experimental curve has an infinite number of points, and therefore, a parametrization of the curve is required to characterize and capture the behaviour of the tissue. The MLTs were trained providing the five material parameters of the SEF defined by the GOH model [15]. The performance of both inputs (parameters of the double exponential and customized parameters) was initially compared using ANNs, and then the method of the extraction of three customized parameters (initial slope, middle point and final slope) from the stress-strain curves, which was the most effective method, was used for the subsequent training. Therefore, the two proposed fitting methods were trained repetitively until convergence, and this was carried out by considering a different number of neurons in the hidden layers. After that, the other machine learning tools were built and trained. This part is the application stage.

The verification stage considers the five outputs of the previous stage as new equation inputs in order to check the performance of the application. First, a validation with new observations of analytical curves (previously unseen observations by the MLT) was performed, following which the tool was re-validated with two kinds of experimental data; (i) experimental data of a coronary artery (adventitia layer) obtained by Holzapfel *et. al* [8] and (ii) uniaxial test data from a carotid artery of swine obtained previously by our research group [44]. Simple tension tests on the circumferential and axial strips of the swine vessels were performed with a high precision drive Instron Microtester 5548 system adapted for biological specimens [44]. Different loading and unloading cycles were applied corresponding to approximately 120 [kPa] Engineering stress level at 30%/min of strain rate. Several cycles were applied in order to precondition the sample. The last cycle was used in the subsequent stress-stretch analysis. The Cauchy stress in the direction of the stretch was computed as $\sigma_{\theta\theta,zz} = \frac{F_{\theta,z}}{t_{\theta,z} w_{\theta,z}} \lambda_{\theta,z}$, where F is the load registered by the Instron machine and $t_{\theta,z}$ and $w_{\theta,z}$ are the initial thickness and width, and $\lambda_{\theta,z}$ is the stretch in circumferential and longitudinal directions respectively measured by the video-extensometer.

Accepted Article

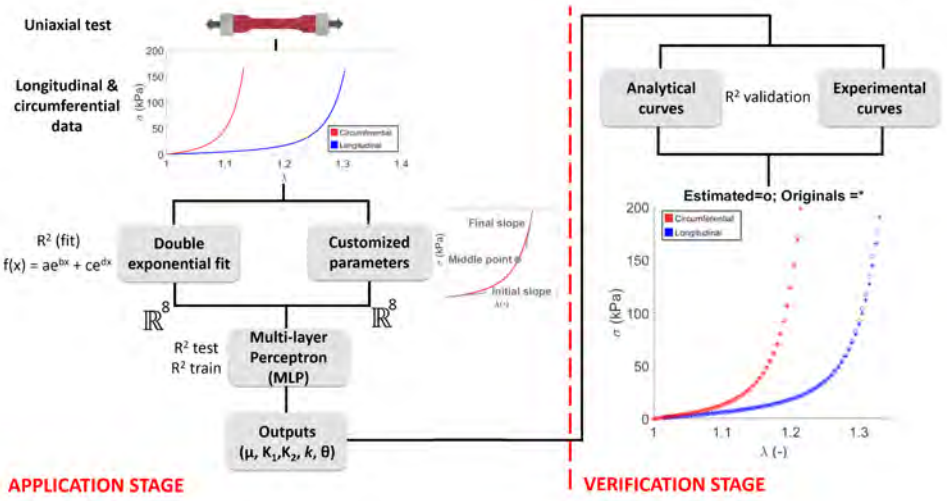

Figure 1. Workflow for the application and verification stages.

The assessment of models was carried out by using the well-known coefficient of determination, R^2: the closer this value is to 1, the better the fitting becomes. Moreover, the assessment of relative errors (REs) for both training and testing sets was considered necessary in order to show the efficiency in finding correlations between inputs and outputs. By doing so, it is possible to determine the quality of the training stage (higher performances for lower training error) as well as the ability of the predictive phase (higher performance for a lower testing error).

$$R^2 = \frac{\sigma_{\hat{\theta}\theta}}{\sigma_{\hat{\theta}}\sigma_{\theta}}, \tag{10}$$

$$RE = abs(\frac{\hat{\theta} - \theta}{\theta}), \tag{11}$$

where $\sigma_{\hat{\theta}\theta}$ is the covariance of the predicted and real values, $\sigma_{\hat{\theta}}$, σ_{θ} the standard deviations of predicted and real values, respectively, and $\hat{\theta}$ and θ the predicted and real values, respectively.

The sample was initially divided into three sets (train (80%), test (10%) and validation(10%)) in order to generate and validate the ANN models. The model was trained using the train set, the test set was used for the determination of the optimal parameters of the model, and the model was validated with the validation test. Thus, the model was validated with an unseen set at the training stage in such a way that the model would be able to predict elements not utilized in its construction.

Accepted Article

In addition, in order to minimize the selection of this validation set, a process of 10-fold cross-validation was implemented [45]. This performs the process described above for 10 iterations, all the elements being used eventually to train or validate the model. Finally, the error rates shown in the pair are the mean values of the selected criteria for these iterations. Additionally, the tool was re-validated with real experimental curves of blood vessels in order to rule out the influence of the sample on the tool performance.

4. RESULTS

The flow diagram shown in Figure 1represents the two stages carried out in this work. Parametrization of the experimental curves was initially implemented using a double exponential function and four customized parameters, namely initial slope, middle point (x, y) and final slope. A preliminary analysis with the ANN achieved better results when fed with customized parameters instead of those coming from the double-exponential fitting. These customized parameters were thus used as the inputs of the three employed algorithms (SVM, Bagged Decision Trees and ANNs) so as to obtain the physical parameters. All the results are displayed in TableI.

The SVM model for regression produced acceptable results when predicting parameters. It should be pointed out that even when values of R^2 are not high (close to 1), they are sufficiently good to establish the output parameters, since in our case the variation of these parameters does not produce a great variation in the generation of the estimated curves.

The results presented in Table I show coefficients of determination (R^2) for both the training and test sets for the Bagged Decision Trees, evaluated with 50, 100 and 500 decision trees at the input. As can be appreciated in Table I, the optimal number of decision trees seems to be 100 (trials with fewer number of decision trees did not work appropriately, so it was decided to select 50 as the lower threshold). For the testing set, 100 trees can thus be considered as the best or optimal solution for this technique not only in terms of computing load, but also for a reasonably accurate model performance since the accuracy criteria become stabilized. Nevertheless, for a higher number of trees (in this case, 500) the method suffers from overfitting. It is therefore possible to achieve reasonable results (coefficients of determination above 0.7 in almost all variables) through this bagged-decision-tree-based technique.

Accepted Article

ANN structures were also tested with the aim of optimizing the model in terms of computational performance and mathematical robustness. For this reason, different networks, with different numbers of artificial neurons, were built and the REs calculated to determine the optimum number of neurons in the hidden layers. In the light of the results gathered in Table II, the optimal number of neurons selected was 20. This was done not only to reduce the computational load but also to maintain the accuracy of the model. In any case, it still presents a coefficient of determination greater than 0.99 for the training stage. For this selected number of neurons, the custom fitting methodology ($R^2_{test} = 0.9945$) obtains better results than the double exponential one ($R^2_{test} = 0.46$) as previously remarked.

Accuracy	SVM for Regression	Bagged Decision Trees		
		No. of decision trees		
		50	100	500
R^2train	0.6566	0.9285	0.9283	0.9331
R^2 test	0.7330	0.7052	0.8062	0.7834

Table I. Accuracy criteria for SVR and Bagged Decision Trees (for three different numbers of trees using a process of 10-fold cross-validation to 1080 pair of curves (circumferential and longitudinal).)

Fitting Type	Accuracy	Number of neurons					
		5	10	20	50	70	100
Custom. fitting	R^2 train	0.9981	0.9999	0.9985	0.9994	0.9989	0.9997
	R^2 test	0.9926	0.9979	0.9945	0.9904	0.9933	0.9956

Table II. Accuracy criteria for the ANN and different numbers of hidden neurons using a process of 10-fold cross-validation to 1080 pair of curves (circumferential and longitudinal).

A verification stage was also implemented by generating estimated curves and comparing them to the original ones. This stage can be initiated after the optimal model has been selected (Figure 1), that is, for the Bagged Decision Trees, an optimal number of 100 and the customized parameters; for the ANN, 20 neurons in the hidden layer and again the model with the customized parameters. The Support Vector Machine for Regression was directly applied without any modification at the input.

By using the estimated parameters provided by the Support Vector Machine for Regression, it was possible to obtain some curves through the analytical process described in the previous sections. An unseen set of data was employed in order to generate new curves with the SVMs, with the aim of validating the tool. After that, the curves obtained were compared with the estimated ones. It is also possible to compare the original and estimated material parameters, as presented in Figure 2.

Accepted Article

Bagged (Bootstrap-Aggregated) Decision Trees with three different numbers of trees at the input (50, 100 and 500) were also implemented to predict the parameters. The datasets were divided into two groups each: training and testing sets. The results presented in Figure 2 show that this method yields, in a very similar way, reasonably good results.

The ANN has been used in a similar fashion: with the estimated parameters provided by this tool, several curves were plotted. Figure 2 shows two particular cases, with different degrees of anisotropy, of the validation process. In view of the customized parameters, this fitting was finally selected due to its excellent mathematical response in terms of the coefficient of determination. These cases correspond to this curve parametrization. The results in Figure 2 show that the ANN is capable of achieving a good fitting of the experimental data for both highly-anisotropic and quasi-isotropic mechanical responses. In addition, due to the fact that the initial slope of the curve is one of the three parameters used to represent each curve, the fitting ability at lower strains is better than that corresponding to the optimization using classical methodology (double exponential) which usually fails to fit at small strains where there is a high stiffening of the curve.

Table III shows the results corresponding to the mean accuracy of the cases presented in Figure 2, in terms of the coefficient of determination, for functions coming from the testing set and both for circumferential and longitudinal cases. It is worth mentioning that all cases exceed a value of 0.99.

Fitting Type	Accuracy	Anisotropic response	Quasi-isotropic response
ANN	R^2 longitudinal	0.9982	0.9989
	R^2 circumferential	0.9962	0.9981
SVM for Regression	R^2 longitudinal	0.9982	0.9989
	R^2 circumferential	0.9962	0.9981
Bagged Decision Trees	R^2 longitudinal	0.9974	0.9998
	R^2 circumferential	0.9998	0.9986

Table III. Assessment of all fittings for highly-anisotropic and quasi-isotropic curves

Finally, the tool was also validated with the real experimental curves of two kinds of blood vessels; coronary artery (Figure 3.a) [8] and carotid artery (Figure 3.b) [44]. The results were again very satisfactory, the behaviour of these biological tissues being well captured by the different machine learning tools. These examples were also fitted by using the customized curve parametrization.

Table IV shows the coefficient of determination of the two cases presented in Figure 3. The R^2 circumferential and longitudinal are also very close to 1, confirming the quality of the fitting.

Accepted Article

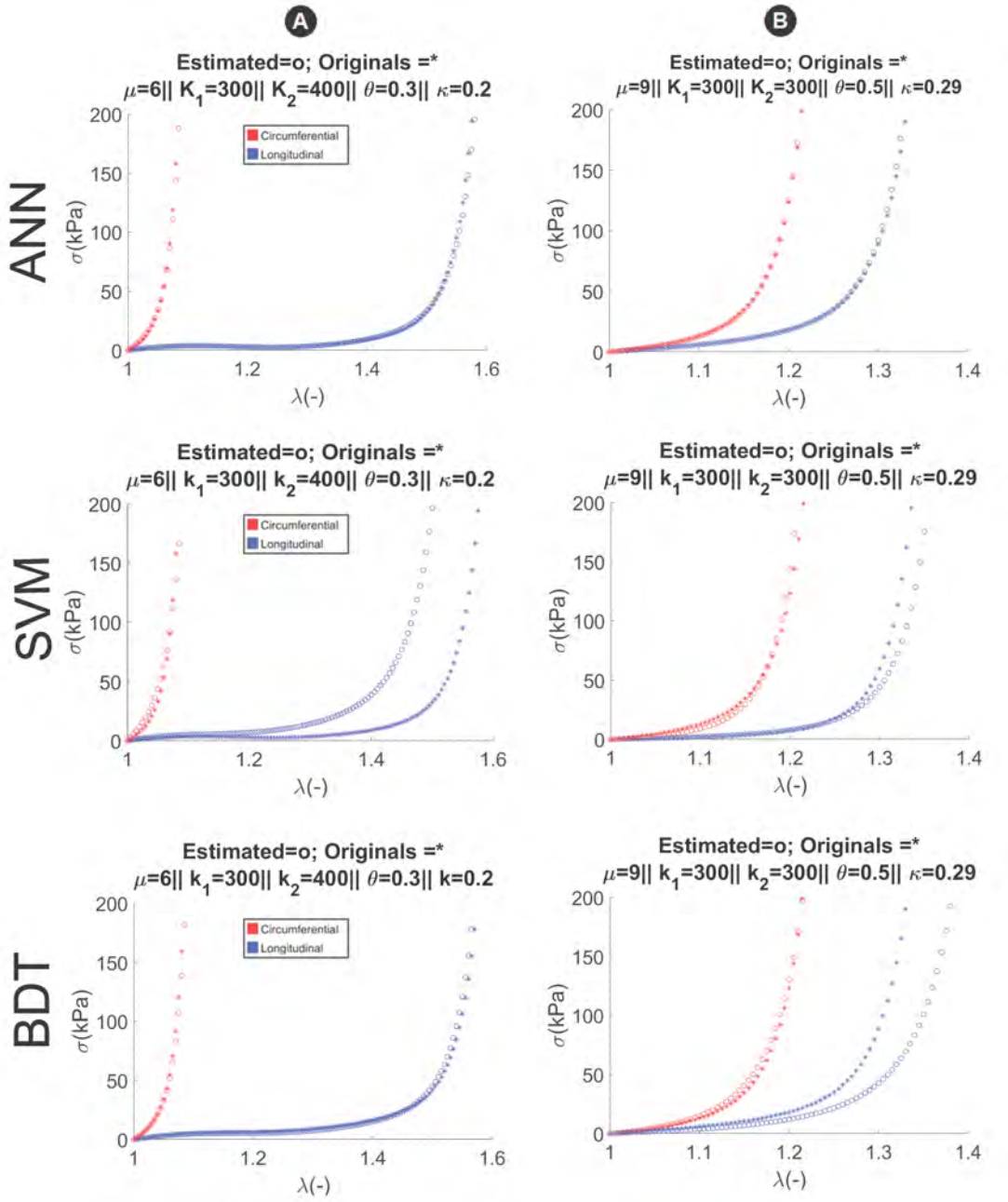

Figure 2. Comparison of estimated (circular markers) and real (asterisk markers) curves. (a) Anisotropic behaviour and (b) quasi-isotropic response for the three methods.

Fitting Type	Accuracy	Coronary artery	Carotid artery
ANN	R^2 Longitudinal	0.983	0.964
	R^2 circumferential	0.992	0.99
SVM for Regression	R^2 Longitudinal	0.96	0.83
	R^2 circumferential	0.89	0.979
Bagged Decision Trees	R^2 Longitudinal	0.98	0.971
	R^2 circumferential	0.991	0.992

Table IV. Assessment of the three fittings for coronary and carotid arteries.

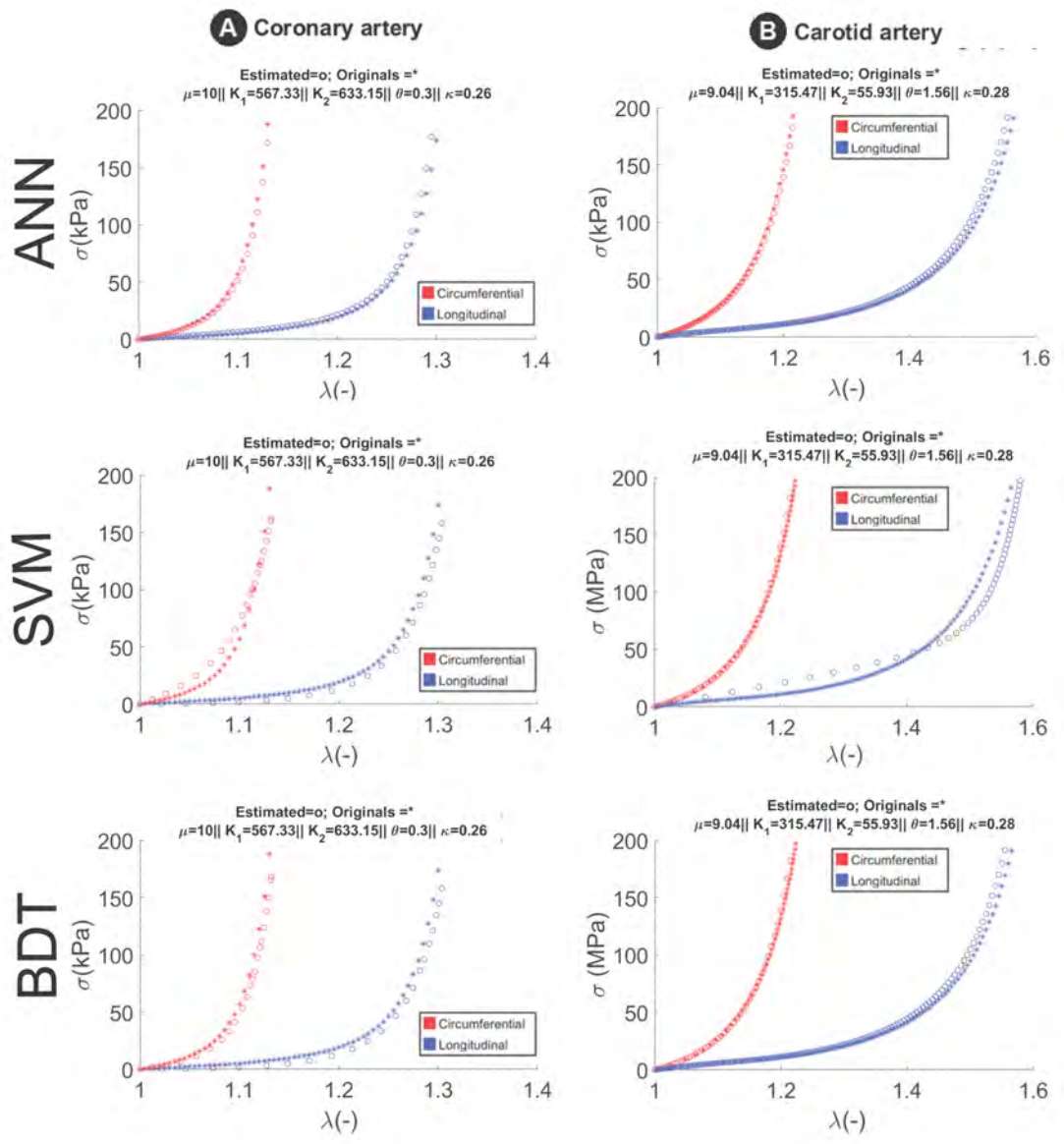

Figure 3. Comparison of estimated (circular markers) and real (asterisk markers) curves for experimental tests of a (a) coronary artery [8] and a (b) carotid artery [44].

5. CONCLUSIONS

In this study, we have investigated whether a constitutive model based on a SEF can be fitted using different MLTs, namely: an Artificial Neural Network, a Support Vector Machine for Regression, and Bagged (Bootstrap-Aggregated) Decision Trees. Uniaxial experimental tests, performed both in circumferential and longitudinal directions, were used for this purpose. The fitting of uniaxial experimental data is usually done using a Levenberg-Marquardt non-linear least square fitting algorithm [16] which minimizes an objective function. Given the well-known problem of numerical methods based on gradients for the fitting of a material model, that is, their limitation to local optimization and, therefore, their instability and dependence on the selected initial seed, three

numerical and complex algorithms based on MLTs have been proposed. These techniques have been previously used to solve different problems in biomechanics, such as the geometry optimization of a short stem hip implant to reduce stress shielding at the proximal femur [30] or the prediction of an atheroma plaque rupture [34]. However, the potential of this technique to accurately obtain the material parameters of the SEF of soft biological tissues, such as the SEF proposed by Gasser, Ogden and Holzapfel (GOH) [15], has never before been investigated. Here, we show that the use of these complex mathematical algorithms could be an alternative to traditional mathematical optimization algorithms based on gradients.

The use of MLTs also has an important advantage in terms of computational costs. The computation training time for the ANN was 15 ± 1 minutes for an optimal number of neurons (once the optimal parameters had been chosen by a k-fold cross validation), and the response time when a new case is evaluated is negligible since ANNs only evaluate one function, providing an immediate estimated response. However, when a method based on gradients such as the least square fitting algorithm [16] is used, an indefinite amount of time is wasted in finding the appropriate initial seed.

This study confirms that it is possible to obtain a good fit of uniaxial experimental curves in a reasonably simple way. It has been demonstrated that the use of only three simple parameters (initial slope, middle point and final slope) per each family of curves (circumferential and longitudinal directions), which can also be computed from the experimental data in a very simple way, could be a good approach of the curves. The parameters could therefore be used to get a good fitting of the experimental curves within a short computational time.

Although the aforementioned results are very interesting and promising, this study has some limitations. A particular issue concerns the observed variability for the real curves: it might be necessary to consider the study of new analytical or customized parametrizations which would potentially provide better results. In addition, the complexity of the model and the techniques used require simpler approaches. In this way, the capabilities for testing the methodology in real cases might be enhanced.

Nevertheless, despite these limitations and given the results obtained, it is certainly reasonable to conclude that MLTs are able to replace gradient methods of optimization to fit the material parameters in the uniaxial experimental testing of soft biological tissue samples. In addition, the methodology proposed in this work for uniaxial tests could be easily extended to other kinds of experimental techniques such as biaxial or inflation tests.

Accepted Article

6. ACKNOWLEDGEMENTS

Acknowledgements for the research support from the Spanish Ministry of Economy, Industry and Competitiveness through the research project TIN2016-76770-R and DPI2016-76630-C2-1-R, and the CIBER-BBN initiative. The experimental tests were performed by the ICTS "NANBIOSIS", specifically by the Tissue and Scaffold Characterization Unit (U13) of the CIBER in Bioengineering, Biomaterials and Nanomedicine (CIBER-BBN at the University of Zaragoza).

7. BIBLIOGRAPHY

REFERENCES

1. Fung Y. C., Fronek K., Patitucci P.. Pseudoelasticity of arteries and the choice of its mathematical expression. *American Journal of Physiology.* 1979;237:620-631.
2. Fung Y. C.. *Biomechanics. Mechanical properties of living tissues*. Springer-Verlag; 1990.
3. Humphrey J. D.. Stress, strain, and mechanotransduction in cells. *ASME Journal of Biomechanical Engineering.* 2001;123(6):638-641.
4. Hayashi K., Washizu T., Tsushima N., Kiraly R. J., Nose Y.. Mechanical properties of aortas and pulmonary arteries of calves implanted with cardiac prostheses.. *Journal of Biomechanics.* 1981;14(3):173-182.
5. Hayashi K., Imai H.. Tensile property of atheromatous plaque and an analysis of stress in atherosclerotic wall. *Journal of Biomechanics.* 1997;30:573-579.
6. Schulze-Bauer C. A. J., Mrth C., Holzapfel G. A.. Passive biaxial mechanical response of agel human iliac arteries. *ASME Journal of Biomechanical Engineering.* 2003;125:395-406.
7. Holzapfel G. A., Stadler M., Gasser C. T.. Changes in the mechanical environment of stenotic arteries during interaction with stents: Computational assessment of parametric stent designs. *ASME Journal of Biomechanical Engineering.* 2005a;127:166-180.
8. Holzapfel G. A., Gasser C. T., Sommer G., Regitnig P.. Determination of the layer-specific mechanical properties of human coronary arteries with non-atherosclerotic intimal thickening, and related constitutive modelling. *American Journal of Physiology - Heart and Circulatory Physiology.* 2005b;289:2048-2058.
9. Ogden R. W.. Nonlinear elasticity, anisotropy, material stability and residual stresses in soft tissues. *Biomechanics of Soft Tissue in Cardiovascular Systems. CISM Courses and Lectures.* 2003;441:65-108.
10. Truesdell C., Noll W.. *The Non-Linear Field Theories of Mechanics*. Springer-Verlag, 3rd edition; 2004.
11. Demiray H.. A note on the elasticity of soft biological tissues. *Journal of Biomechanics.* 1972;5:309-311.
12. Humphrey J. D., Yin F. C.. A new constitutive formulation for characterizing the mechanical behavior of soft tissues. *Biophysical Journal.* 1987;53(4):564-570.
13. Weiss J. A., Maker B. N., Govindjee S.. Finite element implementation of incompressible, transversely isotropic hyperelasticity. *Computer Methods in Applied Mechanics and Engineering.* 1996;135:107-128.
14. Holzapfel G. A., Gasser T. C., Ogden R. W.. A new constitutive framework for arterial wall mechanics and a comparative study of material models. *Journal of Elasticity.* 2000;61:1-48.

Accepted Article

15. Gasser T. Christian, Ogden Ray W., Holzapfel Gerhard A.. Hyperelastic modelling of arterial layers with distributed collagen fibre orientations. *Journal of The Royal Society of Interface.* 2006;3:15–35.
16. Marquardt D. W.. An algorithm for least-squares estimation of nonlinear parameters. *SIAM Journal on Applied Mathematics.* 1963;11:431-441.
17. Avril S., Evans S.. *Material Parameter Identification and Inverse Problems in Soft Tissue Biomechanics*. CISM International Centre for Mechanical Sciences; 2017.
18. McCulloch W. S, Pitts W. S. A logical calculus of the ideas inmanent in nervous activity. *Bulletin of Mathematical Biophysics.* 1943;5:115-133.
19. Gurney K.. *An introduction to neural networks*. London: Routledge; 1997.
20. Jabbour K.. *Automated load forecasting assistant*. Proceedings of the IEEE Power Engineering Society Summer Meeting; 1987.
21. Evans B., Fisher D.. *Process delay analyses using decision-tree induction*. Technical report CS92-06, Department of Computer Science, Vanderbilt University, Nashville, Tennessee; 1992.
22. Taboada J., Matas J. M., Ordez C., Garca P. J.. Creating a quality map of a slate deposit using support vector machines. *Journal of Computational and Applied Mathematics.* 2007;204:84-94.
23. Lpez M., Martnez J., Matas J. M., Taboada J., Viln J. A.. Functional classification of ornamental stone using machine learning techniques. *Journal of Computational and Applied Mathematics.* 2010;234:1338-1345.
24. Fayyad U. M., Weir N., Djorgovski S.. A machine learning system for automated cataloging of large scale sky surveys. *Proceedings of the Tenth International Conference on Machine Learning and Applications.*. 1993;1:112-119.
25. Liu Y.H., Chang F., Lin C.C.. Language Identification of Character Images Using Machine Learning Techniques. *Document Analysis and Recognition, International Conference on.* 2005;1:630-634.
26. Handels H., Rob Th., Kreusch J., Wolff H. H., Poopl S. J.. A feature selection for optimized skin tumor recognition using genetic algorithms. *Artificial Intelligence in Medicine.* 1999;16:283-297.
27. Gniadecka M., Alshede P.P, Sigurdsson S., Wessel S.. Melanoma diagnosis by Raman spectroscopy and neural networks: Structure alterations in proteins and lipids in intact cancer tissue. *Journal of Investigative Dermatology.* 2004;122:443-449.
28. Huang Ming, Kecman Vojislav. Gene extraction for cancer diagnosis by support vector machines. *Artificial Intelligence in Medicine.* 2005;35:185-194.
29. Garijo N., Martnez J., Garca-Aznar J.M., Prez M.A.. Computational evaluation of different numerical tools for the prediction of proximal femur loads from bone morphology. *Computer Methods in Applied Mechanics and Engineering.* 2014;268(Supplement C):437 - 450.
30. Cilla M., Borgiani E., Martnez J., Duda G.N., Checa S. Machine learning techniques for the optimization of joint replacements: Application to a short-stem hip implant. *PLOS ONE.* 2017;12(9):1-16.
31. Poli R., Cagnoni S., Livi R., Coppini G., Valli G.. A neural network expert system for diagnosing and treating hypertension. *Computer.* 1991;3:64-71.
32. Itchhaporia D., Almassy R., Kaufman L., Snow P., Oetgen W.. Artificial neural networks can predict significant coronary disease. *Journal of the American College of Cardiology.* 1995;25:328.
33. Itchhaporia D., Snow P.B., Almassy R.J., Oetgen W.J.. Artificial neural networks: Current status in cardiovascular medicine. *Journal of the American College of Cardiology.* 1996;28(2):515-521.
34. Cilla M., Martnez J., Pea E., Martnez M. A.. Machine Learning Techniques as a helpful tool towards determination of plaque vulnerability. *IEEE Transactions on Biomedical Engineering.* 2012b;9(4):1155-1161.
35. Liang L., Kong F., Martin C., et al. Machine learning-based 3-D geometry reconstruction and modeling of aortic valve deformation using 3-D computed tomography images. *International Journal for Numerical Methods in Biomedical Engineering.* 2017;33(5).
36. Spencer A. J. M.. Theory of invariants. *Continuum physics. Academic Press, New York.* 1971;:239-253.

Accepted Article

37. Bishop C. M.. *Neural networks and pattern recognition*. Oxford University Press; 1995.
38. Vapnik V.. The support vector method of function estimation. *Neural Networks and Machine Learning.* 1998;1:239-268.
39. Antkowiak M.. *Artificial neural networks vs. support vector machines for skin diseases recognition*. Master's Thesis in Computing Science, Umea University, Sweden; 2006.
40. Garca-Nieto P.J., Martnez J., Arajo M., Ordez C.. Support vector machines and neural networks used to evaluate paper manufactured using Eucalyptus globulus. *Applied Mathematical Modelling.* 2012;36(12):6137-6145.
41. James G., Witten D., Hastie T., Tibshirani R.. *An introduction to Statistical Learning*. Springer; 2013.
42. Kononenko I.. Machine learning for medical diagnosis: History, state of the art and perspective. *Artificial Intelligence in Medicine.* 2001;23(1):89-109.
43. Fan F., Cong W., Wang G.. A new type of neurons for machine learning. *International Journal for Numerical Methods in Biomedical Engineering.* 2018;34:e2920.
44. Garca A., Pea E., Laborda A., et al. Experimental study and constitutive modelling of the passive mechanical properties of the porcine carotid artery and its relation to histological analysis. Implications in animal cardiovascular device trials. *Medical Engineering & Physics.* 2011;33:665-676.
45. Stone M.. Cross-Validatory Choice and Assessment of Statistical Predictions. *Journal of Royal Statistical Society Eries B.* 1974;36:111-147.

Accepted Article